# Impact of water sediment diversion and afflux on erosion deposition in the Luoshan Hankou reach, 1 middle Yangtze River, China

# Impact of water-sediment diversion and afflux on erosion-deposition in the Luoshan-Hankou reach, middle Yangtze River, China

Boyuan Zhu[a,b,*], Jianhao Qin[a,b], Yitian Li[c], Gexuanzi Luo[d], Qi Xu[a,b], Lingfeng Liu[a,b], Alistair G.L. Borthwick[e,f]

[a] School of Hydraulic and Environmental Engineering, Changsha University of Science & Technology, Changsha 410114, China

[b] Key Laboratory of Water-Sediment Sciences and Water Disaster Prevention of Hunan Province, Changsha 410114, China

[c] State Key Laboratory of Water Resources and Hydropower Engineering Science, Wuhan 430072, China

[d] Changsha Institute of Mining Research CO, LTD, Changsha 410012, China

[e] School of Engineering, The University of Edinburgh, The King's Buildings, Edinburgh EH9 3JL, UK

[f] School of Engineering, Computing and Mathematics, University of Plymouth, Plymouth PL4 8AA, UK

Corresponding author: Boyuan Zhu (email: boyuan@csust.edu.cn)

**Abstract**

It is not yet fully understood how water-sediment diversion and afflux along a mainstream reach of a river affect erosion-deposition in downstream reaches. This study focuses on the Luoshan-Hankou mainstream reach of the middle Yangtze River, China. The Luoshan-Hankou reach is vitally important for flood control, being located downstream of three diversion mouths and an afflux outlet along the Jingjiang reach. We establish empirical formulae for sediment transport rates at boundary cross-sections, and hence estimate the amount and proportion of erosion-deposition and its relative increase (termed erosion-deposition promotion) in the Luoshan-Hankou reach. We then propose critical net water supplies from Dongting Lake to Luoshan-Hankou reach based on maxima and equilibria of erosion-deposition and its promotion. It is found that net water supply partly drives erosion-deposition in the Luoshan-Hankou reach where maximal proportions of deposition and deposition-promotion may be approximated by $0.01c^{-37.67}$ and $0.01c^{-37.67}+c-1$ in which $c$ is a dimensionless parameter representing the erosion-deposition condition in Luoshan-Hankou reach for no water-sediment exchange. At Zhicheng hydrological station, the critical ratio of net water supply to overall water discharge is $0.418c^{-33.33}-1$, and critical net water supply ratios for equilibria of erosion-deposition and its promotion are -1 (or $c^{-33.33}-1$) and 0 (or $(0.06+3.257c^{54.61})^{-1}-1$). A chart based on net water supply and $c$ is devised representing four types of erosion-deposition and its promotion for the Luoshan-Hankou reach. Historical data over the past 65 years demonstrate that erosion-deposition and its promotion in the reach are respectively governed by $c$ and net water supply; there is a remarkable shift from alternate erosion-deposition to monotonic erosion whilst the erosion-deposition effect remains consistent. The foregoing are in agreement with observed data, and comparable with data for the Jingjiang reach (affected by the three water-sediment diversion mouths). Satisfactory flood-control conditions in the convergence zone between the Yangtze mainstream and Dongting Lake accompanied by increasing erosion in the Luoshan-Hankou reach are predicted for the future.

**Keywords:** Luoshan-Hankou reach; Dongting Lake; Water-sediment exchange; Erosion-deposition;

Erosion-deposition promotion

## 1. Introduction

Water and sediment diversions from a river into distributaries, and affluxes from tributaries into a river affect net erosion-deposition in mainstream reaches. This can have engineering consequences, such as altered flood risk, navigation obstruction and land-resource loss. In China, water diversion for agricultural irrigation along the Kubuqi (Hobq) Desert reach of the Yellow River as it passes through Inner Mongolia has caused the mainstream flow velocity to decrease, enhancing sediment deposition and raising the mainstream flood discharge level (Pan et al., 2015). In the US, large-scale sediment diversion along the lower Mississippi River, through distributaries or small canals to restore sub-deltas, has diminished the deposition rate in mainstream reaches, lowering flood flow lines and effectively reducing navigation-related dredging volumes (Kemp et al., 2014). In South America, the decreasing trend in sediment afflux from the Madeira River (a major tributary of the Amazon River) has partly triggered muddy coast degradation and increased the risk of wetland recession in the Amazon Estuary (Li et al., 2020). Several previous studies have quantitatively dissected the influence mechanism of water-sediment diversion and afflux on erosion-deposition in a river mainstream (Lindner, 1953; Kerssens and Van Urk, 1986; Wang and Yin, 1989). To data, the focus has been on cases where either diversion or afflux solely occurs. However, there is a need to understand how the river mainstream evolves in cases where diversion and afflux occur concurrently along a given river. This is especially pertinent at the present time as many large rivers worldwide are experiencing intense human interference from dam construction, water-soil conservation works, sand excavation, etc.

The Yangtze River, China, has received widespread attention regarding erosion-deposition of its riverbed. The Luoshan-Hankou reach is located in the middle Yangtze River, immediately downstream of a water-sediment diversion and afflux system between Jingjiang reach and Dongting Lake, and occupies ~ 90% of the length of the Chenglingji-Hankou reach whose net erosion-deposition is of major concern owing to its

critical impact on local flood control, especially near Chenglingji at the afflux outlet of Dongting Lake (Zhou, 2005; Han, 2006; Han et al., 2017). A major debate has taken place as to whether net sediment erosion or deposition would occur in the Chenglingji-Hankou reach after the impoundment of the Three Gorges Dam (TGD). One view (Zhou, 2005) was that riverbed evolution of the Chenglingji-Hankou reach was primarily determined by the amount of coarse sediment (of median diameter $d > 0.1$ mm) entering the reach. Given that the Jingjiang reach had experienced substantial sediment erosion after the impoundment of the TGD and thence supplied abundant coarse sediment to the Chenglingji-Hankou reach, it was most likely that persistent (> 100 years) sediment deposition would occur in the Chenglingji-Hankou reach. Another study (Han, 2006) argued that the Chenglingji-Hankou reach had experienced both sediment erosion and deposition after impoundment of the TGD, with erosion resulting from the sediment trapping effect of the TGD, and deposition from the settling out of eroded material from the Jingjiang reach and a reduction in sediment diversion from the Jingjiang reach into Dongting Lake. This latter argument placed emphasis on the bed-forming effects of both fine ($d < 0.1$ mm) and coarse ($d > 0.1$ mm) sediment present in the river. Later researches demonstrate that the Chenglingji-Hankou reach has indeed experienced erosion after the impoundment of the TGD (Yuan et al., 2012; Han et al., 2017; Guo et al., 2019).

The Luoshan-Hankou reach exhibits similar riverbed evolution characteristics to those of the Chenglingji-Hankou reach and also acts as a key river segment for flood control, motivating many studies of its net erosion-deposition (Fang et al., 2012; Dai and Liu, 2013; Han et al., 2017; Lai et al., 2017; Dai Z J et al., 2018; Yang et al., 2018; Guo et al., 2019). The foregoing agree that the Luoshan-Hankou reach has changed from a sediment-sink before the impoundment of the TGD to a sediment-source after, during which time the TGD-induced sharp reduction in sediment delivery downstream has played the dominant role, expedited by water-soil conservation and sand extraction activities (Dai and Liu, 2013; Dai et al., 2018). Meanwhile, the TGD has smoothed downstream hydrologic processes, thus altering the geomorphological evolution of bed features, such as mid-channel bars, in this reach (Mei et al., 2015; Lou et al., 2018).

Although the TGD is the determining factor behind erosion-deposition in the Luoshan-Hankou reach, it has also been observed that water-sediment diversion and afflux between the Jingjiang reach and the Dongting Lake also contribute (Han, 2006; Mei et al., 2015; Dai Z J et al., 2018). Specifically, Dongting Lake is not only receiving decreased water-sediment through diversion from the Jingjiang reach while facilitating the entry of additional mainstream water and sediment into the Luoshan-Hankou reach (Han, 2006), but has also weakened the flattening effect of the TGD on hydrological behavior in this reach (Mei et al., 2015). Moreover, the lake has also changed from a sediment-sink to a sediment-source (Dai et al., 2018) since TGD impoundment. The foregoing necessarily modulate water and sediment budgets in the Luoshan-Hankou reach and affect its riverbed erosion-deposition. Nevertheless, previous studies have mainly focused on variations in water-sediment diversion and afflux and corresponding erosion-deposition changes in the Dongting Lake area (Chang et al., 2010; Ou et al., 2014; Yang et al., 2014; Zhang et al., 2015; Zhu et al., 2015; Li et al., 2016; Wang et al., 2017; Yu et al., 2018). To date, little attention has been paid to the impact of water-sediment diversion and afflux on riverbed erosion-deposition in the Luoshan-Hankou reach.

Hu et al. (2016) carried out a relevant study of the Jingjiang reach which overlaps the three diversion mouths and is located upstream of the afflux outlet of Dongting Lake at Chenglingji. Specifically, Hu et al. (2016) discovered that the water-sediment diversions inherently promote deposition in adjacent mainstream reaches. However, this deposition-promotion has attenuated in recent decades due to the decreasing discharge trend in the water-sediment diversions, with an average deposition-promotion ratio of ~20% achieved during 1957-2010. (The deposition-promotion ratio is defined as the proportion of increased sediment deposition caused by the water-sediment diversions, accounted in the sediment flux entering the Jingjiang reach.) The Luoshan-Hankou reach receives water and sediment from the upstream Jingjiang reach (after water-sediment diversion and afflux have occurred) and the Hanjiang River (a tributary of the Yangtze River) (Zhou, 2005; Han, 2006; Han et al., 2017; Yang et al., 2018), and so undoubtedly undergoes a

different erosion-deposition response to changes in systemic water-sediment exchanges between the Jingjiang reach and the Dongting Lake.

The present study explores the net erosion-deposition response of the Luoshan-Hankou reach to changes in water-sediment diversion and afflux along the Jingjiang reach, based on integrated data on daily water-sediment discharges at selected hydrological stations and multi-year average net erosion-deposition in the Luoshan-Hankou reach over the past 65 years (1955-2019), afforced by sediment-budget computations at prescribed cross-sections. Critical water-sediment exchange conditions are deduced for erosion-deposition and its relative increase (termed erosion-deposition promotion) in the Luoshan-Hankou reach, and an assessment chart devised that delineates four types of erosion-deposition condition. Historical variations of erosion-deposition and its promotion are calculated, and key influence factors identified. Erosion-deposition promotion effects of water-sediment diversion and afflux on the Luoshan-Hankou and Jingjiang reaches are compared, erosion-deposition types to be avoided in the Luoshan-Hankou reach are proposed, and an assessment made of the future flood situation in the reach. This paper quantifies the reaction of riverbed erosion-deposition processes to distributary diversion and tributary afflux along part of the middle Yangtze mainstream, and deepens our knowledge of the interaction between the Yangtze mainstream and Dongting Lake. Our research findings are instructive for water-sediment regulation and regional flood-control in the convergence zone between the Yangtze River and Dongting Lake, and might be applicable to other river-lake connection systems that are also undergoing complex variations in water-sediment exchanges.

## 2. Geographical setting

The Luoshan-Hankou reach is situated in the middle Yangtze River, stretching 251 km from Luoshan hydrological station to Hankou hydrological station (Figs. 1a and 1b), and connects to the Hanjiang River, a tributary of the Yangtze River (Figs. 1a and 1b)). The Jingjiang reach is located 31 km upstream of the Luoshan-Hankou reach and extends 347 km from Zhicheng hydrological station to the outlet of Dongting Lake at Chenglingji (Fig. 1b). Three water-sediment diversion mouths at Songzikou, Taipingkou and

Ouchikou, are distributed along the south bank of the Jingjiang reach (Fig. 1b). The Jingjiang reach is divided into upper and lower segments according to the location of Ouchikou (Fig. 1b). Water and sediment in the upper Jingjiang segment are diverted into Dongting Lake through the three mouths, and after redistribution in Dongting Lake and mixing with inflows from four tributaries at the southwest of the lake (i.e. Xiangjiang River, Zijiang River, Yuanjiang River, and Lishui River), water and sediment flow back into the Yangtze mainstream at Chenglingji (Fig. 1b). In short, water and sediment in the Luoshan-Hankou reach are supplied from three sources: (1) the upper entrance of the Jingjiang reach after deduction of fluxes through the three diversion mouths and some replenishment of afflux at Chenglingji, (2) eroded riverbed material from the Jingjiang and Chenglingji-Luoshan reaches, and (3) the Hangjiang River.

Water and sediment discharges entering the Jingjiang reach and the Luoshan-Hankou reach are recorded at Zhicheng and Luoshan hydrological stations, and those flowing out of the Luoshan-Hankou reach are recorded at Hankou hydrological station (Figs. 1a and 1b). Water and sediment discharges at the three diversion mouths along the south bank of the upper Jingjiang reach are recorded at five hydrological stations in the distributaries. Diversion discharges at Songzikou are evaluated as the sum of flow records obtained at Xinjiangkou and Shadaoguan hydrological stations, those at Taipingkou are acquired from Mituosi hydrological station, and those at Ouchikou are calculated as the sum of records from Kangjiagang and Guanjiapu hydrological stations (Fig. 1b). Water and sediment data from the afflux at Chenglingji and from the Hanjiang River are respectively recorded at Qilishan and Xiantao hydrological stations (Fig. 1b). Water and sediment discharges within the Yangtze mainstream interval between Ouchikou and Chenglingji are recorded at Jianli hydrological station (Figs. 1a and 1b). Data on daily water and sediment time series at the foregoing hydrological stations and multi-year average net erosion-deposition of the Luoshan-Hankou reach over the past 65 years (1955-2019) were acquired from the Changjiang Water Resources Commission (including the Changjiang Sediment Bulletin during 2000-2019, URL: http://www.cjw.gov.cn/zwzc/bmgb/nsgb/List_1.html).

## 3. Methods

### *3.1. Identification of impact of water-sediment diversion and afflux on net erosion-deposition in Luoshan-Hankou reach*

Fig. 2 is a schematic diagram of the Yangtze mainstream side of the river-lake connection system from Zhicheng to Hankou. To identify the impact of the three water-sediment diversions and single afflux on net erosion-deposition in the Luoshan-Hankou reach, sediment transport rates at the two boundaries of the reach are estimated for two cases: Case I, the actual reach with water-sediment diversion and afflux; and Case II, the idealized reach without any water-sediment diversion and afflux. In the middle Yangtze River, sandy bedload accounts for less than 5% of the total sediment discharge (Xia et al., 2016; Han et al., 2017) and so we ignore its effect on riverbed erosion-deposition. The present study considers solely the transport of suspended sediment load.

The afflux outlet of the Hanjiang River is very close to the downstream boundary of the Luoshan-Hankou reach (Figs. 1 and 2). Moreover, water and sediment discharges from the Hanjiang River only account for ~ 5% and ~ 10% of the mainstream discharges at the multi-year average scale (Table S1). Thus, water and sediment affluxes from the Hanjiang River hardly interfere with net erosion-deposition in the Luoshan-Hankou reach, and so are not taken into consideration.

In fluvial rivers, hydrodynamic factors such as flow velocity and water depth are mainly determined by the incoming water discharge. Therefore, the sediment transport rate is usually expressed as a function of water discharge (Qian et al., 1987; Hu et al., 2016). However, extreme flood events and human activities, especially dam construction associated with substantial sediment trapping, can cause severe fluctuations in the riverine sediment concentration. This inevitably disrupts the relatively stable relationship between sediment transport rate and water discharge. By introducing the sediment concentration at an adjacent upstream cross-section, we avoid this kind of problem. Hence, the sediment transport rate at a given

cross-section, $G$ (in kg/s), is described by the following power function (Wang and Yin, 1989; Lu et al., 2012):

$$G = KQ^{\alpha}S^{\beta} \tag{1}$$

where $Q$ (in $m^3/s$) is the water discharge at the cross-section, $S$ (in $kg/m^3$) is sediment concentration at an adjacent upstream cross-section, $K$ is a coefficient, and $\alpha$ and $\beta$ ($\alpha > 1$) are exponents whose sum is approximately 2. It should be noted that there cannot be water-sediment diversion and afflux between the cross-section and the adjacent upstream cross-section when using this equation. Moreover, Eq. (1) neglects sand excavation effects. However, the total amount of sand excavated from the middle Yangtze is less than 5% of the amount eroded from the riverbed (Dai and Liu, 2013), indicating that sand excavation has little impact on the sediment transport rate in the Luoshan-Hankou reach.

Sediment transport rates are estimated through multiplication of water discharge and sediment concentration values from data continuously recorded at Luoshan and Hankou hydrological stations. However, the data cannot be used to directly quantify general expressions for erosion-deposition and its promotion in the Luoshan-Hankou reach or for the corresponding critical conditions of water-sediment exchanges between the Yangtze mainstream and Dongting Lake according to the maxima and equilibria of erosion-deposition and its promotion. Moreover, measurements of water discharge and sediment concentration are unavailable for the two stations considered in Case II. Given that $K$, $\alpha$ and $\beta$ in Eq. (1) can be calibrated using the measured data at these two stations and their values remain roughly constant for Cases I and II (Wang and Yin, 1989; Lu et al., 2012; Hu et al., 2016), Eq. (1) offers a practical approach by which to estimate the sediment transport rate at these stations. Calibration of the coefficient and exponents of Eq. (1) is based on its transform:

$$G = KQ^{\alpha}S^{2-\alpha} \tag{2}$$

which may be rearranged to give

$$\frac{G}{S^2} = K\left(\frac{Q}{S}\right)^{\alpha} \tag{3}$$

Eq. (3) is fitted to measured data on $Q$, $S$ and their product, $G$, at relevant stations and cross-sections to determine values for $K$ and $\alpha$, noting that $\beta$=2-$\alpha$.

*3.1.1 . Case I: Actual reach with water-sediment diversion and afflux*

We denote the ratio of the sum of water discharges at the three diversion mouths along the Jingjiang reach to that at Zhicheng station as $\eta_{TDM}$, and the ratio of water discharge at Qilishan station to that at Zhicheng station as $\eta_{Qilishan}$, and estimate the sediment concentration at Cross-section 1-1 (a mainstream cross-section immediately downstream of Chenglingji, Fig. 2) from:

$$S_1 = \frac{Q_{Jianli}S_{Jianli} + Q_{Qilishan}S_{Qilishan}}{Q_{Jianli} + Q_{Qilishan}} \tag{4}$$

where $Q_{Jianli}$ (in $m^3/s$), $Q_{Qilishan}$ (in $m^3/s$), $S_{Jianli}$ (in $kg/m^3$) and $S_{Qilishan}$ (in $kg/m^3$) are water discharges and sediment concentrations at Jianli and Qilishan stations. Sediment transport rates at Luoshan and Hankou stations, $G_{Luoshan}$ (in kg/s) and $G_{Hankou}$ (in kg/s), are then calculated as:

$$G_{Luoshan} = K_{Luoshan}\left\{\left[1+\left(\eta_{Qilishan}-\eta_{TDM}\right)\right]Q_{Zhicheng}\right\}^{\alpha_{Luoshan}} S_1^{\beta_{Luoshan}} \tag{5}$$

$$G_{Hankou} = K_{Hankou}\left\{\left[1+\left(\eta_{Qilishan}-\eta_{TDM}\right)\right]Q_{Zhicheng}\right\}^{\alpha_{Hankou}} S_{Luoshan}^{\beta_{Hankou}} \tag{6}$$

where $Q_{Zhicheng}$ (in $m^3/s$) and $S_{Luoshan}$ (in $kg/m^3$) are the water discharge and sediment concentration at Zhicheng and Luoshan stations, $K_{Luoshan}$ and $K_{Hankou}$ are coefficients, and $\alpha_{Luoshan}$, $\alpha_{Hankou}$, $\beta_{Luoshan}$ and $\beta_{Hankou}$ are power exponents obtained for the Luoshan and Hankou stations.

Hence, the net erosion-deposition rate in the actual Luoshan-Hankou reach, $\Delta G_{Luoshan-Hankou}$ (in kg/s) is determined as:

$$\begin{aligned}\Delta G_{Luoshan-Hankou} &= G_{Luoshan} - G_{Hankou} \\ &= K_{Luoshan}\left\{\left[1+\left(\eta_{Qilishan}-\eta_{TDM}\right)\right]Q_{Zhicheng}\right\}^{\alpha_{Luoshan}} S_1^{\beta_{Luoshan}} - K_{Hankou}\left\{\left[1+\left(\eta_{Qilishan}-\eta_{TDM}\right)\right]Q_{Zhicheng}\right\}^{\alpha_{Hankou}} S_{Luoshan}^{\beta_{Hankou}}\end{aligned} \tag{7}$$

Given that the net sediment supply ratio from Dongting Lake to the Luoshan-Hankou reach partially correlates with $\eta_{Qilishan}$-$\eta_{TDM}$, and its impact on erosion-deposition in Luoshan-Hankou reach is contained in

$S_1$ and $S_{Luoshan}$ (mainstream sediment concentrations after water-sediment exchanges between Dongting Lake and the Yangtze mainstream), the net sediment supply ratio does not feature explicitly in the foregoing empirical formulae and subsequent analyses.

*3.1.2. Case II: Idealized reach without water-sediment diversion and afflux*

In this case, water discharges at Luoshan and Hankou stations approximate that at Zhicheng station, and sediment concentrations at Cross-section 1-1 and Luoshan station are roughly equal to $S_1$ and $S_{Luoshan}$ (Text S1). Thus, the sediment transport rates at Luoshan and Hankou stations, $G'_{Luoshan}$ (in kg/s) and $G'_{Hankou}$ (in kg/s), are expressed as:

$$G'_{Luoshan} = K_{Luoshan} Q_{Zhicheng}^{\alpha_{Luoshan}} S_1^{\beta_{Luoshan}} \tag{8}$$

$$G'_{Hankou} = K_{Hankou} Q_{Zhicheng}^{\alpha_{Hankou}} S_{Luoshan}^{\beta_{Hankou}} \tag{9}$$

Accordingly, the net erosion-deposition rate in the idealized Luoshan-Hankou reach, $\Delta G'_{Luoshan-Hankou}$ (in kg/s), is obtained as:

$$\begin{aligned} \Delta G'_{Luoshan-Hankou} &= G'_{Luoshan} - G'_{Hankou} \\ &= K_{Luoshan} Q_{Zhicheng}^{\alpha_{Luoshan}} S_1^{\beta_{Luoshan}} - K_{Hankou} Q_{Zhicheng}^{\alpha_{Hankou}} S_{Luoshan}^{\beta_{Hankou}} \end{aligned} \tag{10}$$

*3.1.3. Comparison between Case I and Case II*

In accordance with previous studies (Lu et al., 2012; Hu et al., 2016), the proportion of net erosion-deposition in the actual Luoshan-Hankou reach to the sediment discharge entering the idealized Luoshan-Hankou reach, $\varphi$, is given by:

$$\begin{aligned} \varphi &= \frac{\Delta G_{Luoshan-Hankou}}{G'_{Luoshan}} \\ &= \left[1+\left(\eta_{Qilishan}-\eta_{TDM}\right)\right]^{\alpha_{Luoshan}} - \frac{K_{Hankou}}{K_{Luoshan}} \left[1+\left(\eta_{Qilishan}-\eta_{TDM}\right)\right]^{\alpha_{Hankou}} Q_{Zhicheng}^{\alpha_{Hankou}-\alpha_{Luoshan}} \frac{S_{Luoshan}^{\beta_{Hankou}}}{S_1^{\beta_{Luoshan}}} \end{aligned} \tag{11}$$

The difference in net erosion-deposition rates between the actual and the idealized Luoshan-Hankou reaches, namely the net erosion-deposition rate caused by the water-sediment diversion and afflux along the Jingjiang reach, $\delta_{Luoshan-Hankou}$ (in kg/s), is deduced from:

$$\begin{aligned}\delta_{Luoshan-Hankou} &= \Delta G_{Luoshan-Hankou} - \Delta G'_{Luoshan-Hankou} \\ &= K_{Luoshan} Q_{Zhicheng}^{\alpha_{Luoshan}} S_1^{\beta_{Luoshan}} \left\{ \left[ 1 + \left( \eta_{Qilishan} - \eta_{TDM} \right) \right]^{\alpha_{Luoshan}} - 1 \right\} + K_{Hankou} Q_{Zhicheng}^{\alpha_{Hankou}} S_{Luoshan}^{\beta_{Hankou}} \left\{ 1 - \left[ 1 + \left( \eta_{Qilishan} - \eta_{TDM} \right) \right]^{\alpha_{Hankou}} \right\}\end{aligned} \tag{12}$$

The proportion of this net erosion-deposition difference accounted in the sediment discharge entering the idealized Luoshan-Hankou reach, $\psi$, which we call the net erosion-deposition promotion ratio, is determined from:

$$\begin{aligned}\psi &= \frac{\delta_{Luoshan-Hankou}}{G'_{Luoshan}} \\ &= \left\{ \left[ 1 + \left( \eta_{Qilishan} - \eta_{TDM} \right) \right]^{\alpha_{Luoshan}} - 1 \right\} + \frac{K_{Hankou}}{K_{Luoshan}} Q_{Zhicheng}^{\alpha_{Hankou} - \alpha_{Luoshan}} \frac{S_{Luoshan}^{\beta_{Hankou}}}{S_1^{\beta_{Luoshan}}} \left\{ 1 - \left[ 1 + \left( \eta_{Qilishan} - \eta_{TDM} \right) \right]^{\alpha_{Hankou}} \right\}\end{aligned} \tag{13}$$

To simplify Eqs. (11) and (13), a dimensionless parameter, $c$, is introduced to represent the erosion-deposition condition of the idealized Luoshan-Hankou reach as:

$$c = \frac{K_{Hankou} Q_{Zhicheng}^{\alpha_{Hankou}} S_{Luoshan}^{\beta_{Hankou}}}{K_{Luoshan} Q_{Zhicheng}^{\alpha_{Luoshan}} S_1^{\beta_{Luoshan}}} \tag{14}$$

where $c = 1$, $c > 1$, and $c < 1$ imply sediment balance, erosion, and deposition in the idealized Luoshan-Hankou reach. Herein, $c$ represents the contributions to erosion-deposition in the Luoshan-Hankou reach from changes in mainstream water and sediment discharges driven by natural factors (e.g. precipitation, basin sediment yield and upper reach erosion-deposition) and human interference (e.g. dam construction and water-soil conservation).

Then, Eqs. (11) and (13) are rewritten as:

$$\varphi = \left[ 1 + \left( \eta_{Qilishan} - \eta_{TDM} \right) \right]^{\alpha_{Luoshan}} - c \left[ 1 + \left( \eta_{Qilishan} - \eta_{TDM} \right) \right]^{\alpha_{Hankou}} \tag{15}$$

$$\psi = \left\{ \left[ 1 + \left( \eta_{Qilishan} - \eta_{TDM} \right) \right]^{\alpha_{Luoshan}} - 1 \right\} + c \left\{ 1 - \left[ 1 + \left( \eta_{Qilishan} - \eta_{TDM} \right) \right]^{\alpha_{Hankou}} \right\} \tag{16}$$

### *3.2. Critical values of $\eta_{Qilishan}$-$\eta_{TDM}$*

We consider four critical values. The first critical value of $\eta_{Qilishan}$-$\eta_{TDM}$, corresponding to the sediment erosion-deposition equilibrium of the actual Luoshan-Hankou reach, is determined from $\varphi = 0$ and denoted as $(\eta_{Qilishan}\text{-}\eta_{TDM})_1$. The second critical value of $\eta_{Qilishan}$-$\eta_{TDM}$, corresponding to the largest value of $\varphi$ (denoted as $\varphi_m$), is determined from $\dfrac{d\varphi}{d\left(\eta_{Qilishan} - \eta_{TDM}\right)} = 0$ and denoted as $(\eta_{Qilishan}\text{-}\eta_{TDM})_2$. The third critical

value of $\eta_{Qilishan}$-$\eta_{TDM}$, corresponding to the conversion from a deposition-promotion effect to an erosion-promotion effect of water-sediment diversion and afflux along the Jingjiang reach on net erosion-deposition in the actual Luoshan-Hankou reach, is determined from $\psi = 0$ and denoted as $(\eta_{Qilishan}$-$\eta_{TDM})_3$. The fourth critical value of $\eta_{Qilishan}$-$\eta_{TDM}$, corresponding to the largest value of $\psi$ (denoted as $\psi_m$), is determined from $\frac{d\psi}{d\left(\eta_{Qilishan}-\eta_{TDM}\right)}=0$ and denoted as $(\eta_{Qilishan}$-$\eta_{TDM})_4$.

## 4. Results

### *4.1. Erosion-deposition response of the actual Luoshan-Hankou reach to water diversion and afflux along the Jingjiang reach*

The actual Luoshan-Hankou reach experiences an overall trend from sediment erosion to deposition as $\eta_{TDM}$ increases (Fig. 3a) and from sediment deposition to erosion as $\eta_{Qilishan}$ and $\eta_{Qilishan}$-$\eta_{TDM}$ increase (Figs. 3b and 3c). In other words, higher $\eta_{TDM}$ corresponds to decreased Yangtze mainstream discharge entering the actual Luoshan-Hankou reach, whereas higher $\eta_{Qilishan}$ and $\eta_{Qilishan}$-$\eta_{TDM}$ indicate an increased net water supply from Dongting Lake, respectively resulting in lower and higher sediment transport capacities (Tan et al., 2018) in the reach, and exacerbating the severity of deposition-promotion and erosion-promotion effects. Moreover, erosion-deposition in the actual Luoshan-Hankou reach exhibits tighter correlation with $\eta_{Qilishan}$-$\eta_{TDM}$ than with individual $\eta_{TDM}$ or $\eta_{Qilishan}$, as indicated by the higher value of $R$ and lower value of $P$ in Fig. 3c than in Figs. 3a and 3b, implying that $\eta_{Qilishan}$-$\eta_{TDM}$ is more effective than separate water diversion or afflux in driving erosion-deposition processes in the actual Luoshan-Hankou reach, especially given that $P<0.05$ in Fig. 3c. Nonetheless, many other factors also affect erosion-deposition of the reach; the $R$ and $P$ values in Fig. 3c remain unsatisfactory, stimulating evaluation of the $\eta_{Qilishan}$-$\eta_{TDM}$ contribution in the present study.

### *4.2. Calibrated K, α, β, calculated φ, ψ, $\varphi_m$, $\psi_m$, and corresponding critical $\eta_{Qilishan}$-$\eta_{TDM}$ values*

Fig. 4 shows the calibrated values of $K_{Luoshan}$, $\alpha_{Luoshan}$, $K_{Hankou}$, and $\alpha_{Hankou}$ using daily measured data of

297 water discharge and sediment concentration at relevant stations and cross-sections throughout 1956-2019 for
298 Luoshan and 1961-2019 for Hankou. It can be seen from Figs. S2 and S3 that the calibrated values of the
299 coefficients and exponents remain roughly stable during pre-TGD and post-TGD periods. Moreover, the
300 high values of $R$ and low values of $P$ in Figs. 4, S2 and S3 indicate tight correlations. Therefore, we adopt
301 values of $K_{Luoshan}$, $\alpha_{Luoshan}$, $K_{Hankou}$ and $\alpha_{Hankou}$ that are calibrated using data covering the whole period,
302 namely 0.26, 1.13, 0.17 and 1.16 in Fig. 4, from which we estimate $\beta_{Luoshan}$ to be 0.87 and $\beta_{Hankou}$ to be 0.84.
303 These calibrated parameter values produce high consistency between the calculated and measured sediment
304 transport rates at Luoshan and Hankou stations (Fig. S4). Moreover, the values are similar to previously
305 published values for the middle Yangtze River (Qian et al., 1987; Hu et al., 2016).

306 Table 1 lists empirical relationships for $\varphi$, $\psi$, $\varphi_m$, $\psi_m$ as functions of $c$ and $\eta_{Qilishan}$-$\eta_{TDM}$. Empirical
307 formulae for determining critical values of $\eta_{Qilishan}$-$\eta_{TDM}$ are also supplied. Fig. 5 displays the correlation
308 between $\varphi/\psi$ and $\eta_{Qilishan}$-$\eta_{TDM}$ for different $c$ values.

309 It can be deduced from Table 1 and Fig. 5a that:

310 (1) For $c < 0.94$, the actual Luoshan-Hankou reach always experiences deposition. For $c \geq 0.94$, the
311 actual Luoshan-Hankou reach undergoes deposition when $-1 < \eta_{Qilishan}\text{-}\eta_{TDM} < (c^{-33.33}\text{-}1)$ and erosion when
312 $\eta_{Qilishan}\text{-}\eta_{TDM} > (c^{-33.33}\text{-}1)$. Moreover, if $\eta_{Qilishan}\text{-}\eta_{TDM} = -1$ or $(c^{-33.33}\text{-}1)$ (i.e. $(\eta_{Qilishan}\text{-}\eta_{TDO})_1$), the actual
313 Luoshan-Hankou reach remains in a state of erosion-deposition equilibrium for all $c$ values.

314 (2) For each $c$ value, $\varphi$ of the actual Luoshan-Hankou reach increases progressively with $\eta_{Qilishan}$-$\eta_{TDM}$
315 until it attains a peak of $\varphi_m = 0.010c^{-37.67}$ (i.e. the most severe deposition state) at $\eta_{Qilishan}\text{-}\eta_{TDM} =$
316 $(0.418c^{-33.33}\text{-}1)$, after which $\varphi$ declines with further increase in $\eta_{Qilishan}$-$\eta_{TDM}$.

317 (3) Erosion-deposition in the actual Luoshan-Hankou reach is closely related to that of the idealized
318 Luoshan-Hankou reach. The more deposition occurs in the idealized Luoshan-Hankou reach (i.e. the lower
319 the value of $c$), the more deposition (including maximum deposition) and less erosion are experienced by the
320 actual Luoshan-Hankou reach. Therefore, higher $\varphi$ values are obtained under the deposition condition ($c < 1$)

of the idealized Luoshan-Hankou reach than under its erosion condition ($c > 1$). Furthermore, the value of $\eta_{Qilishan}$-$\eta_{TDM}$ (i.e. $(\eta_{Qilishan}$-$\eta_{TDO})_2$) associated with maximum deposition in the actual Luoshan-Hankou reach is larger under more severe deposition conditions (i.e. lower $c$ values) in the idealized Luoshan-Hankou reach than under slight deposition or erosion conditions (i.e. higher $c$ values).

It can be deduced from Table 1 and Fig. 5b that:

(1) For $0.93 \leq c \leq 1$, water-sediment exchanges between the Jingjiang reach and Dongting Lake exert no impact on erosion-deposition in the actual Luoshan-Hankou reach (i.e. $\psi = 0$) when $\eta_{Qilishan}$-$\eta_{TDM} = 0$ and $[(0.06+3.257c^{54.61})^{-1}$-1], promote deposition in the actual Luoshan-Hankou reach when $\eta_{Qilishan}$-$\eta_{TDM}$ lies between 0 and $[(0.06+3.257c^{54.61})^{-1}$-1], and facilitate erosion in the actual Luoshan-Hankou reach when $\eta_{Qilishan}$-$\eta_{TDM}$ has a value outside the range $\{0, [(0.06+3.257c^{54.61})^{-1}$-1]$\}$. For $c < 0.93$ or $c > 1$, $\psi$=0 when $\eta_{Qilishan}$-$\eta_{TDM} = 0$. Deposition-promotion prevails when $\eta_{Qilishan}$-$\eta_{TDM} > 0$ and erosion-promotion prevails when $\eta_{Qilishan}$-$\eta_{TDM} < 0$ for $c < 0.93$. Conversely, deposition-promotion dominates when $\eta_{Qilishan}$-$\eta_{TDM} < 0$ and erosion-promotion dominates when $\eta_{Qilishan}$-$\eta_{TDM} > 0$ for $c > 1$.

(2) Maximum deposition-promotion (i.e. $\psi_m$) occurs at $\eta_{Qilishan}$-$\eta_{TDM} = 0.418c^{-33.33}$-1 for all $c$ values.

(3) For $\eta_{Qilishan}$-$\eta_{TDM} > 0$, lower $c$ values correspond to higher $\psi$ values, suggesting that more severe deposition in the idealized Luoshan-Hankou reach usually triggers a more significant deposition-promotion effect in the actual Luoshan-Hankou reach after water-sediment exchanges between the Jingjiang reach and the Dongting Lake. For $\eta_{Qilishan}$-$\eta_{TDM} < 0$, the situation reverses.

*4.3. A chart for assessing erosion-deposition and its promotion in the actual Luoshan-Hankou reach*

Fig. 6 plots the functions $(\eta_{Qilishan}$-$\eta_{TDM})_1 = -1$, $(\eta_{Qilishan}$-$\eta_{TDM})_1 = c^{-33.33}$-1, $(\eta_{Qilishan}$-$\eta_{TDM})_2 = 0.418c^{-33.33}$-1, $(\eta_{Qilishan}$-$\eta_{TDM})_3 = 0$, $(\eta_{Qilishan}$-$\eta_{TDM})_3 = (0.06+3.257c^{54.61})^{-1}$-1 and $(\eta_{Qilishan}$-$\eta_{TDM})_4 = 0.418c^{-33.33}$-1 with respect to $c$. The curves traced by $(\eta_{Qilishan}$-$\eta_{TDM})_1 = -1$, $(\eta_{Qilishan}$-$\eta_{TDM})_1 = c^{-33.33}$-1, $(\eta_{Qilishan}$-$\eta_{TDM})_3 = 0$, and $(\eta_{Qilishan}$-$\eta_{TDM})_3 = (0.06+3.257c^{54.61})^{-1}$-1 divide the diagram into 6 subareas, which in turn are classified as 4 erosion-deposition and erosion-deposition promotion types.

**Subarea I ($\eta_{Qilishan}$-$\eta_{TDM}$ > 0 and $\eta_{Qilishan}$-$\eta_{TDM}$ > $c^{-33.33}$-1):** erosion and erosion-promotion **(Type I)**. The actual Luoshan-Hankou reach experiences both erosion and erosion-promotion driven by water-sediment exchanges between the Jingjiang reach and Dongting Lake.

**Subareas II (0 < $\eta_{Qilishan}$-$\eta_{TDM}$ < $c^{-33.33}$-1 and $(0.06+3.257c^{54.61})^{-1}$-1 <$\eta_{Qilishan}$-$\eta_{TDM}$ < $c^{-33.33}$-1) and IV (-1 < $\eta_{Qilishan}$-$\eta_{TDM}$ < 0 and -1 < $\eta_{Qilishan}$-$\eta_{TDM}$ < $(0.06+3.257c^{54.61})^{-1}$-1):** deposition and erosion-promotion **(Type II)**. Although the actual Luoshan-Hankou reach experiences deposition when $\eta_{Qilishan}$-$\eta_{TDM}$ is located in these two subareas, such deposition is suppressed by water-sediment exchanges between the Jingjiang reach and the Dongting Lake. Moreover, the idealized Luoshan-Hankou reach also undergoes deposition (i.e. $c < 1$) in these two subareas.

**Subareas III (0 < $\eta_{Qilishan}$-$\eta_{TDM}$ < $(0.06+3.257c^{54.61})^{-1}$-1) and V ($(0.06+3.257c^{54.61})^{-1}$-1 < $\eta_{Qilishan}$-$\eta_{TDM}$ < 0 and -1 < $\eta_{Qilishan}$-$\eta_{TDM}$ < $c^{-33.33}$-1):** deposition and deposition-promotion **(Type III)**. The actual Luoshan-Hankou reach undergoes both deposition and deposition-promotion owing to water-sediment exchanges between the Jingjiang reach and Dongting Lake. Importantly, when $\eta_{Qilishan}$-$\eta_{TDM}$ is situated along the curve described by $(\eta_{Qilishan}\text{-}\eta_{TDM})_2 = (\eta_{Qilishan}\text{-}\eta_{TDM})_4 = 0.418c^{-33.33}\text{-}1$, deposition and deposition-promotion are most severe. Furthermore, the idealized Luoshan-Hankou reach also experiences deposition (i.e. $c < 1$) in Subarea III.

**Subarea VI ($c^{-33.33}$-1 < $\eta_{Qilishan}$-$\eta_{TDO}$ < 0):** erosion and deposition-promotion **(Type IV)**. Although the actual Luoshan-Hankou reach witnesses erosion, this is hindered by water-sediment exchanges between the Jingjiang reach and Dongting Lake. The idealized Luoshan-Hankou reach also undergoes erosion (i.e. $c > 1$) in Subarea VI.

*4.4. Historical changes in river-lake water exchange and variables related to erosion-deposition in the Luoshan-Hankou reach*

Fig. 7 shows that the total water diversion at the three mouths along the Jingjiang reach and the water afflux at Qilishan station have experienced synchronous decreases over the past 65 years, resulting in overall

stable but yearly fluctuating net water supply and $\eta_{Qilishan}$-$\eta_{TDM}$ from Dongting Lake into the actual Luoshan-Hankou reach.

Based on Fig. 7, variables related to erosion-deposition in the actual Luoshan-Hankou reach are evaluated. Table 2 lists the results, which demonstrate that:

(1) Due to net water supply from Dongting Lake, the actual Luoshan-Hankou reach underwent consistent erosion-promotion throughout all the periods of interest. This finding is also supported by the correlations in Figs. 3b and 3c.

(2) Considering net erosion-deposition, the actual Luoshan-Hankou reach experienced alternating prevalent deposition and inferior erosion processes before 2003, but underwent continuous erosion after 2003 under the significant sediment trapping effect of the TGD (Yuan et al., 2012; Dai and Lu, 2014; Han et al., 2017; Guo et al., 2019). Moreover, $\Delta G_{Luoshan\text{-}Hankou}$ presented an acceptable approximation to $T$, indicating that Eq. (7) could effectively calculate net erosion-deposition in the actual Luoshan-Hankou reach.

(3) Based on the linear regression equations in Table 2, erosion-deposition and its promotion respectively depended on $c$ and $\eta_{Qilishan}$-$\eta_{TDM}$. Consequently, while the actual Luoshan-Hankou reach experienced an overall change from alternate erosion and deposition events to monotonic erosion conditions as $c$ increased under the sharp reduction in incoming sediment from the upstream reach, it also underwent an erosion-promotion effect with no obvious unidirectional trend, given the relatively stable value of $\eta_{Qilishan}$-$\eta_{TDM}$.

(4) $\eta_{Qilishan}$-$\eta_{TDM}$, $c$ and calculated $\varphi$ and $\psi$ during the periods of interest were mainly located in Subareas I and II of Fig. 6. This not only verifies Fig. 6, but also implies that the actual Luoshan-Hankou reach encounters two major conditions at the multi-year average scale: erosion and erosion-promotion, and deposition and erosion-promotion.

## 5. Discussion

*5.1. Erosion-deposition promotion in different mainstream reaches*

The Luoshan-Hankou reach is located downstream of three diversion mouths and an afflux outlet, which are overlapped by the Jingjiang reach (Figs. 1b and 2). Discrepancies therefore occur in the erosion-deposition promotions produced by the mainstream-lake water and sediment exchanges in the two Yangtze mainstream reaches. Erosion-deposition promotion in the Luoshan-Hankou reach is determined by the net water supply from the Dongting Lake. Water afflux at Chenglingji is generally larger than the sum of water diversions at the three mouths (Fig. 7), and so erosion-promotion persists in the Luoshan-Hankou reach and even alters the reach from sediment deposition condition to erosion conditions as $\eta_{Qilishan}$-$\eta_{TDM}$ increases (Fig. 3c). Over the past decades, $\eta_{Qilishan}$-$\eta_{TDM}$ has fluctuated, causing erosion-promotion also to fluctuate (Table 2). By comparison, erosion-deposition promotion in the Jingjiang reach depends on water diversion at the three mouths, which reduces the water discharge and weakens the sediment carrying capacity of the mainstream, leading to consistent deposition-promotion in the reach (Hu et al., 2016). Under the decreasing trend in water-diversion discharge, deposition-promotion has correspondingly declined (Hu et al., 2016). In terms of erosion-deposition promotion ratio, the multi-year average $|\psi|$ for the Luoshan-Hankou reach was ~ 10% over the 1959-2019 period (Table 2), whereas that for the mainstream reaches about the three diversion mouths along the Jingjiang reach was ~ 20% over the 1957-2010 period (Hu et al., 2016). If Hu et al. (2016) had focused on the whole Jingjiang reach, we believe that the two $|\psi|$ values would have been more comparable. Similar erosion-deposition promotion events caused by water-sediment diversion and afflux along the mainstream have also been observed in other rivers, such as the Yellow River (Pan et al., 2015), Mississippi River (Kemp et al., 2014; Wang and Xu, 2020), and Amazon River (Li et al., 2020).

A much better understanding is presently needed of erosion-deposition processes in river mainstream reaches located upstream of water-sediment diversion mouths and afflux outlets. It has been speculated that a river mainstream upstream of diversion mouths is prone to suffer erosion-promotion because water

417 diversion steepens the water surface slope and increases the velocity of the mainstream flow, and hence its
418 sediment carrying capacity (Wang and Hu, 2004; Viparelli et al., 2015), whereas a river mainstream reach
419 located upstream of afflux outlets is likely to experience deposition-promotion due to the jacking effects of
420 the water afflux on the water discharge in the mainstream, reducing its water surface slope and flow velocity
421 (Ou et al., 2014; Sun et al., 2014; Chen et al., 2018, 2020). As water diversion or afflux discharges increase,
422 erosion-promotion and deposition-promotion events are likely to be more pronounced.

423 *5.2. Practical use of the assessment chart for erosion-deposition and its promotion*

424 Fig. 6 is useful from a flood-risk management perspective. Subarea I in Fig. 6 reinforces sediment
425 erosion in the Luoshan-Hankou reach, and helps maintain satisfactory flood-control conditions in this reach
426 and the region around Chenglingji. Conversely, subareas III and V, especially those areas in the vicinity of
427 the function curve $(\eta_{Qilishan}\text{-}\eta_{TDM})_2 = (\eta_{Qilishan}\text{-}\eta_{TDM})_4 = 0.418c^{-33.33}\text{-}1$, greatly strengthen sediment deposition
428 and must be avoided. Subareas II and IV suggest a deposition state for both of the actual and idealized
429 Luoshan-Hankou reaches, where deposition is hindered due to the erosion-promotion effect. Therefore, these
430 two subareas are also beneficial for regional flood-control. Subarea VI implies an erosion state for both the
431 actual and idealized Luoshan-Hankou reaches, where erosion is hampered by the deposition-promotion
432 effect. This situation is likely to occur during mainstream flood events when water diversion at the three
433 mouths is largely enhanced (Xia et al., 2014; Li et al., 2016). Although the water afflux at Chenglingji is
434 synchronously augmented at these times by the enhanced discharge at the three diversion mouths and the
435 raised flood water level within Dongting Lake (Fig. 7; Hayashi et al., 2008), this augmentation is restricted
436 by the jacking effect of the high water level in the Yangtze mainstream, resulting in a constringent increase
437 in net water supply from Dongting Lake into the Luoshan-Hankou reach (Chang et al., 2010; Zhan et al.,
438 2015; Dai X et al., 2018). Hence, subarea VI should also be avoided.

439 In Table 2, 1966, 1981, 2003 and 2008 are years in which implementation commenced of the lower
440 Jingjiang Cutoff Projects (Fig. 1b), the impoundment of the Gezhou Dam (Fig. 1), the initial impoundment

of the TGD (Fig. 1) and the experimental impoundment of the TGD. In 1986, the Gezhou Dam ceased to exert further influence on the evolution of the downstream reach (Zhu et al., 2015; Guo et al., 2019). All these major engineering projects have caused riverbed incision along the Jingjiang reach (Xia et al., 2016; Han et al., 2017, 2018). Dam operations have also clipped flood peaks in the reach (Han et al., 2018; Li et al., 2018; Chen et al., 2019). Taken together, these have greatly reduced water diversion from the Jingjiang river into Dongting Lake (Zhang et al., 2015; Zhu et al., 2015; Yu et al., 2018), which has consequently diminished water afflux from Dongting Lake into the Luoshan-Hankou reach over the past decades (Fig. 7). As a result, a relatively stable net water supply has occurred from Dongting Lake to the Luoshan-Hankou reach (Fig. 7). As riverbed incision in the Jingjiang reach weakens (Yuan et al., 2012; Hu et al., 2015; Zhu et al., 2015) and dam-induced flood-peak clip persists (Duan et al., 2016; Han et al., 2018; Zhu et al., 2020), the multi-year average net water supply (i.e. $\eta_{Qilishan}$-$\eta_{TDM}$) is likely to remain at a roughly stable value of ~ 60% in the future. Meanwhile, the state of $c > 1$ that has occurred since 2003 (Table 2) will persist over following decades because of the continuous low sediment influx from the upstream reach under the sediment trapping effect of large cascade reservoirs in the upper Yangtze River (Yang et al., 2014; Guo et al., 2019). Therefore, subarea I in Fig. 6 is most likely to match future behavior in the reach, while also providing a satisfactory regional flood-control condition. If flood control and drought resistance (e.g. prevention of zero-flow events along the three diversion distributaries) within the whole river-lake connection system are comprehensively considered (Hayashi et al., 2008; Han et al., 2017; Wang et al., 2017; Xia et al., 2018), systematic engineering measures, such as construction of sluice gates at the diversion mouths and the afflux outlet, may need to be implemented to regulate water-sediment exchanges between the Yangtze mainstream and Dongting Lake (Wang et al., 2017).

## 6. Conclusion

We present empirical formulae for evaluating the amount and proportion of erosion-deposition and its promotion caused by river-lake water-sediment exchanges in the Luoshan-Hankou reach of the middle

Yangtze River, and deduce critical $\eta_{Qilishan}$-$\eta_{TDM}$ values from Dongting Lake to the reach for the maxima and equilibria of erosion-deposition and its promotion. An erosion-deposition assessment chart, consisting of six subareas, has been devised based on two parameters, $c$ and $\eta_{Qilishan}$-$\eta_{TDM}$. The chart was used to classify erosion-deposition in the Luoshan-Hankou reach into four types. We find that over the past 65 years, the annual value of $\eta_{Qilishan}$-$\eta_{TDM}$ changed slightly whereas the yearly sediment load from the upstream reach reduced sharply after impoundment of the TGD. This has resulted in a complete transformation of the Luoshan-Hankou reach from alternate erosion-deposition conditions before 2003 to monotonic erosion afterwards. Fluctuation was evident in erosion-deposition promotion throughout.

Unlike the consistent deposition-promotion in the Jingjiang reach induced by the three water diversions, erosion-promotion persists in the Luoshan-Hankou reach due to the net water supply from Dongting Lake. Both these kinds of promotion effects are comparable in terms of their ratios. We used the assessment chart to suggest types of erosion-deposition and its promotion that should be either averted or encouraged in the Luoshan-Hankou reach in order to maintain satisfactory flood-control conditions in the convergence zone between the Yangtze mainstream and Dongting Lake. In the future, $\eta_{Qilishan}$-$\eta_{TDM}$ is likely to maintain a roughly constant value of ~ 60%, whereas the sediment load from the upstream reach will continuously decrease, helping to optimize erosion-deposition and its promotion in the Luoshan-Hankou reach, and subsequently ensure proper flood-control conditions in the river-lake connection system.

*CRediT authorship contribution statement*

Design of the research framework: B.Y.Z., J.H.Q., Y.T.L and A.G.L.B. Data collection: B.Y.Z., J.H.Q. and G.X.Z.L. Main analysis of the paper, writing of the main manuscript, and preparation of the Appendix A. Supplementary data: B.Y.Z., J.H.Q., Y.T.L and A.G.L.B. Preparation of figures and tables: G.X.Z.L., Q.X. and L.F.L.

**Declaration of Competing Interest**

The authors declare that they have no known competing financial interests or personal relationships that

could have appeared to influence the work reported in this paper.

**Acknowledgements**

This work was funded by the Natural Science Foundation of Hunan Province (Grant No. 2021JJ40607), the Scientific Research Foundation of Hunan Provincial Education Department (Grant No. 20B021) and the National Natural Science Foundation of China (Grants No. 52071031, 51879198 and 52171245). The authors thank the Changjiang Water Resources Commission for providing hydrologic and terrain data. We are also grateful to the three anonymous reviewers for their insightful suggestions.

**Appendix A. Supplementary data**

Supplementary data associated with this article can be found, in the online version, at

**References**

Chang, J., Li, J.B., Lu, D.Q., Zhu, X., Lu, C.Z., Zhou, Y.Y., Deng, C.X., 2010. The hydrological effect between Jingjiang River and Dongting Lake during the initial period of Three Gorges Project operation. J. Geogr. Sci. 20 (5), 771-786. https://doi.org/10.1007/s11442-010-0810-9.

Chen, F., Chen L., Zhang, W., Han, J.Q., Wang, J.Z., 2019. Responses of channel morphology to flow-sediment variations after dam construction: a case study of the Shashi Reach, middle Yangtze River. Hydrol. Res. 50 (5), 1359-1375. https://doi.org/10.2166/nh.2019.066.

Chen, M.F., Deng, J.Y., Fan, S.Y., Li, Y.T., 2018. Applying energy theory to understand the relationship between the Yangtze River and Poyang Lake. J. Geogr. Sci. 28 (8), 1059-1071. https://doi.org/10.1007/s11442-018-1541-6.

Chen, M.F., Fan, S.Y., Deng, J.Y., Wang, X.P., 2020. Impact of the Three Gorges Dam on Regulation and Storage Capacity of Poyang Lake. J. Landscape Res. 12 (6), 50-55. https://doi.org/10.16785/j.issn1943-989x.2020.6.012.

Dai, S.B., Lu, X.X., 2014. Sediment load change in the Yangtze River (Changjiang): A review. Geomorphology 215, 60-73. https://doi.org/10.1016/j.geomorph.2013.05.027.

Dai, X., Yang, G.S., Wan, R.R., Li, Y.Y., 2018. The effect of the Changjiang River on water regimes of its tributary Lake East Dongting. J. Geogr. Sci. 28 (8), 1072-1084. https://doi.org/10.1007/s11442-018-1542-5.

513 Dai, Z.J., Liu, J.T., 2013. Impacts of large dams on downstream fluvial sedimentation: An example of the Three Gorges
514 Dam (TGD) on the Changjiang (Yangtze River). J. Hydrol. 480, 10-18. https://doi.org/10.1016/j.jhydrol.2012.12.003.
515 Dai, Z.J., Mei, X.F., Darby, S.E., Lou, Y.Y., Li, W.H., 2018. Fluvial sediment transfer in the Changjiang (Yangtze)
516 river-estuary depositional system. J. Hydrol. 566, 719-734. https://doi.org/10.1016/j.jhydrol.2018.09.019.
517 Duan, W.X., Guo, S.L., Wang, J., Liu, D.D., 2016. Impact of cascaded reservoirs group on flow regime in the middle and
518 lower reaches of the Yangtze River. Water 8 (6), 1-21. https://doi.org/ 10.3390/w8060218.
519 Fang, H.W., Han, D., He, G.J., Chen, M.H., 2012. Flood management selections for the Yangtze River midstream after the
520 Three Gorges Project operation. J. Hydrol. 432, 1-11. https://doi.org/10.1016/j.jhydrol.2012.01.042.
521 Guo, L.C., Su, N., Townend, I., Wang, Z.B., Zhu, C.Y., Wang, X.Y., Zhang, Y.N., He, Q., 2019. From the headwater to the
522 delta: A synthesis of the basin-scale sediment load regime in the Changjiang River. Earth-Sci. Rev. 197, 1-19.
523 https://doi.org/10.1016/j.earscirev.2019.102900.
524 Han, J.Q., Sun, Z.H., Li, Y.T., Yang, Y.P., 2017. Combined effects of multiple large-scale hydraulic engineering on water
525 stages in the middle Yangtze River. Geomorphology 298, 31-40. https://doi.org/10.1016/j.geomorph.2017.09.034.
526 Han, J.Q., Sun, Z.H., Li, Y.T., 2018. Distribution of erosion intensity in the Jingjiang reach influenced by the Three Gorges
527 Dam. Earth Surf. Proc. Land. 43, 2654-2665. https://doi.org/10.1002/esp.4423.
528 Han, Q.W., 2006. Only deposition in river reach from Chenglingji to Wuhan after impounding of TGR?——Response on
529 “Discussion on the flood control capacity of the middle Yangtze River after the impoundment of Three Gorges
530 Reservoir”. J. Hydroelectr. Eng. 25 (6), 79-90 (in Chinese with English abstract).
531 https://doi.org/10.3969/j.issn.1003-1243.2006.06.014.
532 Hayashi, S., Murakami, S., Xu, K.Q., Watanabe, M., 2008. Effect of the Three Gorges Dam Project on flood control in the
533 Dongting Lake area, China, in a 1998-type flood. J. Hydro-Environ. Res. 2, 148-163.
534 https://doi.org/10.1016/j.jher.2008.10.002.
535 Hu, C.H., Fang, C.M., Cao, W.H., 2015. Shrinking of Dongting Lake and its weakening connection with the Yangtze River:
536 Analysis of the impact on flooding. Int. J. Sediment Res. 30, 256-262. http://dx.doi.org/10.1016/j.ijsrc.2014.05.001.

Hu, M.Y., Li, Y.T., Zhu, B.Y., Chen, M.F., 2016. Impact on erosion and deposition in main stream by flow and sediment diversion at three outlets along the Jingjiang River. J. Sediment Res. 4, 68-73 (in Chinese with English abstract). https://doi.org/ 10.16239/j.cnki.0468-155x.2016.04.011.

Lai, X., Yin, D., Finlayson, B.L., Wei, T., Li, M., Yuan, W., Yang, S., Dai, Z., Gao, S., Chen, Z., 2017. Will river erosion below the Three Gorges Dam stop in the middle Yangtze? J. Hydrol. 554, 24-31. https://doi.org/10.1016/j.jhydrol.2017.08.057.

Li, S.X., Li, Y.T., Yuan, J., Zhang, W., Chai, Y.F., Ren, J.Q., 2018. The impacts of the Three Gorges Dam upon dynamic adjustment mode alternations in the Jingjiang reach of the Yangtze River, China. Geomorphology 318, 230-239. https://doi.org/10.1016/j.geomorph.2018.06.020.

Li, T., Wang, S., Liu, Y.X., Fu, B.J., Gao, D.X., 2020. Reversal of the sediment load increase in the Amazon basin influenced by divergent trends of sediment transport from the Solimoes and Madeira Rivers. Catena 195, 1-9. https://doi.org/10.1016/j.catena.2020.104804.

Li, Y.Y., Yang, G.S., Li, B., Wang, R.R., Duan, W.L., He, Z., 2016. Quantifying the effects of channel change on the discharge diversion of Jingjiang Three Outlets after the operation of the Three Gorges Dam. Hydrol. Res. 47, 161-174. https://doi.org/10.2166/nh.2016.016.

Lindner, C.P., 1953. Diversion from alluvial streams. Trans. A. S. C. E. 118. https://doi.org/10.1061/TACEAT.0006828.

Lou, Y.Y., Mei, X.F., Dai, Z.J., Wang, J., Wei, W., 2018. Evolution of the mid-channel bars in the middle and lower reaches of the Changjiang (Yangtze) River from 1989 to 2014 based on the Landsat satellite images: impact of the Three Gorges Dam. Environ. Earth Sci. 77 (10), 1-18. https://doi.org/10.1007/s12665-018-7576-2.

Lu, H.W., Wang, Y.G., Shi, H.L., 2012. Study on main techniques of water and sediment resources allocation in irrigation system of the Lower Yellow River. J. Hydrol. Eng. 43 (12), 1405-1412 (in Chinese with English abstract). https://doi.org/10.13243/j.cnki.slxb.2012.12.004.

Kerssens, P.J.M., Urk A.V., 1986. Experimental studies on sedimentation due to water withdrawal. J. Hydraul. Eng.-A. S. C. E. 112 (7), 641-656. https://doi.org/10.1061/(ASCE)0733-9429(1986)112:7(641).

561 Kemp, G.P., Day, J.W., Freeman, A.M., 2014. Restoring the sustainability of the Mississippi River Delta. Ecol. Eng. 65,
562 131-146. https://doi.org/10.1016/j.ecoleng.2013.09.055.
563 Mei, X.F., Dai, Z.J., van Gelder, P.H.A.J.M., Gao, J.J., 2015. Linking Three Gorges Dam and downstream hydrological
564 regimes along the Yangtze River, China. Earth Space Sci. 2(4), 94-106. https://doi.org/10.1002/2014EA000052.
565 Ou, C.M., Li, J.B., Zhou, Y.Q., Cheng, W.Y., Yang, Y., Zhao, Z.H., 2014. Evolution characters of water exchange abilities
566 between Dongting Lake and Yangtze River. J. Geogr. Sci. 24 (4), 731-745. https://doi.org/10.1007/s11442-014-1116-0.
567 Pan, B.T., Guan, Q.Y., Liu, Z.B., Gao, H.S., 2015. Analysis of channel evolution characteristics in the Hobq Desert reach of
568 the Yellow River (1962-2000). Global Planet. Change 135, 148-158. https://doi.org/10.1016/j.gloplacha.2015.10.015.
569 Qian, N., Zhang, R., Zhou, Z.D., 1987. Hydraulic geometry, in: Zhu, S.T. (Ed.), Fluvial Process Theory. Science Press,
570 Beijing, pp. 354-366 (in Chinese).
571 Sun, Z.H., Feng, Q.F., Han, J.Q., Cao, Q.X., 2014. Reasons for heavy deposition of sandbar at confluence of Yangtze River
572 and Han river during autumn flood season of 2011. J. Hydroelectr. Eng. 33 (4), 111-117 (in Chinese with English
573 abstract). https://doi.org/CNKI:SUN:SFXB.0.2014-04-017.
574 Tan, G.M., Fang, H.W., Dey, S., Wu, W.M., 2018. Rui-Jin Zhang's research on sediment transport. J. Hydrol. Eng.-A. S. C.
575 E. 144 (6), 1-6. https://doi.org/10.1061/(ASCE)HY.1943-7900.0001464.
576 Viparelli, E., Nittrouer, J.A., Parker, G., 2015. Modeling flow and sediment transport dynamics in the lowermost Mississippi
577 River, Louisiana, USA, with an upstream alluvial-bedrock transition and a downstream bedrock-alluvial transition:
578 Implications for land building using engineered diversions. J. Geophys. Res.-Earth. 120 (3), 534-563.
579 https://doi.org/10.1002/2014JF003257.
580 Wang, B., Xu, Y.J., 2020. Estimating bed material fluxes upstream and downstream of a controlled large bifurcation - the
581 Mississippi-Atchafalaya River diversion. Hydrol. Process. 34 (13), 2864-2877. https://doi.org/10.1002/hyp.13771.
582 Wang, X.Y., Li, X., Baiyinbaoligao, Wu, Y.H., 2017. Maintaining the connected river-lake relationship in the middle
583 Yangtze River reaches after completion of the Three Gorges Project. Int. J. Sediment Res. 32 (4), 487-494.
584 https://doi.org/10.1016/j.ijsrc.2016.12.001.

585 Wang, Y.G., Yin, X.L., 1989. Theoretical analysis and calculation on distributary-induced deposition. J. Sediment Res. (4),
586 60-66 (in Chinese). https://doi.org/ 10.16239/j.cnki.0468-155x.1989.04.007.
587 Wang, Z.Y., Hu, C.H., 2004. Interactions between fluvial systems and large scale hydro-projects. 9th International
588 Symposium on River Sedimentation, 46-64.
589 Xia, J.Q., Deng, S.S., Lu, J.Y., Xu, Q.X., Zong, Q.L., Tan, G.M., 2016. Dynamic channel adjustments in the Jingjiang Reach
590 of the Middle Yangtze River. Sci. Rep. 6, 1-10. https://doi.org/10.1038/srep22802.
591 Xia, J.Q., Guo, P., Zhou, M.R., Falconer, R.A., Wang, Z.H., Chen, Q., 2018. Modelling of flood risks to people and property
592 in a flood diversion zone. J. Zhejiang Univ.-Sc. A 19 (11), 864-877. https://doi.org/10.1631/jzus.A1800124.
593 Xia, J.Q., Zong, Q.L., Deng, S.S., Xu, Q.X., Lu, J.Y., 2014. Seasonal variations in composite riverbank stability in the
594 Lower Jingjiang Reach, China. J. Hydrol. 519, 3664-3673. https://doi.org/10.1016/j.jhydrol.2014.10.061.
595 Yang, S.L., Milliman, J.D., Xu, K.H., Deng, B., Zhang, X.Y., Luo, X.X., 2014. Downstream sedimentary and geomorphic
596 impacts of the Three Gorges Dam on the Yangtze River. Earth-Sci. Rev. 138, 469-486.
597 https://doi.org/10.1016/j.earscirev.2014.07.006.
598 Yang, Y.P., Zhang, M.J., Sun, Z.H., Han, J.Q., Wang, J.J., 2018. The relationship between water level change and river
599 channel geometry adjustment in the downstream of the Three Gorges Dam. J. Geogr. Sci. 28 (12), 1975-1993.
600 https://doi.org/10.1007/s11442-018-1575-9.
601 Yu, Y.W., Mei, X.F., Dai, Z.J., Gao, J.J., Li, J.B., Wang, J., Lou, Y.Y., 2018. Hydromorphological processes of Dongting
602 Lake in China between 1951 and 2014. J. Hydrol. 562, 254-266. https://doi.org/10.1016/j.jhydrol.2018.05.015.
603 Yuan, W.H., Yin, D.W., Finlayson, B., Chen, Z.Y., 2012. Assessing the potential for change in the middle Yangtze River
604 channel following impoundment of the Three Gorges Dam. Geomorphology 147, 27-34.
605 https://doi.org/10.1016/j.geomorph.2011.06.039.
606 Zhan, L.C., Chen, J.S., Zhang, S.Y., Huang, D.W., Li, L., 2015. Relationship between Dongting Lake and surrounding rivers
607 under the operation of the Three Gorges Reservoir, China. Isot. Environ. Healt. S. 51 (2), 255-270.
608 https://doi.org/10.1080/10256016.2015.1020306.

609 Zhang, R., Zhang, S.H., Xu, W., Wang, B.D., Wang, H., 2015. Flow regime of the three outlets on the south bank of
610 Jingjiang River, China: an impact assessment of the Three Gorges Reservoir for 2003-2010. Stoch. Env. Res. Risk A.
611 29 (8), 2047-2060. https://doi.org/10.1007/s00477-015-1121-6.
612 Zhou, J.J., 2005. Discussion on the flood control capacity of the middle Yangtze River after the impoundment of Three
613 Gorges Reservoir (TGR). J. Hydroelectr. Eng. 24 (1), 25-32 (in Chinese with English abstract).
614 https://doi.org/10.3969/j.issn.1003-1243.2005.01.004.
615 Zhu, B.Y., Yue, Y., Borthwick, A.G.L., Yu, W.J., Liang, E.H., Tang, J.W., Chai, Y.F., Li, Y.T., 2020. Decadal link between
616 longitudinal morphological changes in branching channels of Yangtze estuary and movement of the offshore
617 depo-center. Earth Surf. Proc. Land. 45 (11), 2689-2705. https://doi.org/10.1002/esp.4923.
618 Zhu, L.L., Chen, J.C., Yuan, J., Dong, B.J., 2015. Study on variation trends of flow diversion from Jingjiang River to
619 Dongting Lake. J. Hydroelectr. Eng. 34 (2), 103-111 (in Chinese with English abstract).
620 https://doi.org/JournalArticle/5b3b8070c095d70f00792b3b.
621

## Figure Captions

**Fig. 1.** Overview of the Yangtze basin and the study area. (a) Outline map of the Yangtze basin indicating the location of the study area. (b) Plan view of the study area, which shows the water-sediment diversion and afflux system between the Yangtze River and Dongting Lake, and the geographical extent of the Luoshan-Hankou reach, with major dams, hydrological stations and distributaries/tributaries identified.

**Fig. 2.** Schematic diagram of the Yangtze mainstream side of the river-lake connection system from Zhicheng to Hankou.

**Fig. 3.** Correlations between the net erosion-deposition rate (positive representing deposition and negative representing erosion) of the bankfull channel of the actual Luoshan-Hankou reach and $\eta_{TDM}$ (a), $\eta_{Qilishan}$ (b), and $\eta_{Qilishan}$-$\eta_{TDM}$ (c) based on multi-year average values. In the legends, $n$ is the number of data points, $R$ is correlation coefficient, and $P$ is the significance level of the linear regression analysis.

**Fig. 4.** Power-function regressions between $G_{Luoshan}/S_1^2$ and $Q_{Luoshan}/S_1$ (a) and between $G_{Hankou}/S_{Luoshan}^2$ and $Q_{Hankou}/S_{Luoshan}$ (b) using daily data during 1956-2019 and 1961-2019, respectively. In the legends, $n$ is the number of data points, $R$ is the correlation coefficient, and $P$ is the significance level of the regression analysis.

**Fig. 5.** Variations in $\varphi$ (a) and $\psi$ (b) with $\eta_{Qilishan}$-$\eta_{TDM}$ for different $c$ values.

**Fig. 6.** Chart for assessing erosion-deposition and its promotion in the actual Luoshan-Hankou reach, consisting of 6 subareas classified into 4 types.

**Fig. 7.** Yearly water discharge time series at the three diversion mouths along the Jingjiang reach and the afflux outlet at

Chenglingji (a), and associated proportions accounted at Zhicheng station (b) over the past 65 years, from which the yearly net water supply and $\eta_{Qilishan}$-$\eta_{TDM}$ from the Dongting Lake into the actual Luoshan-Hankou reach are obtained.

649 **Fig. 1**

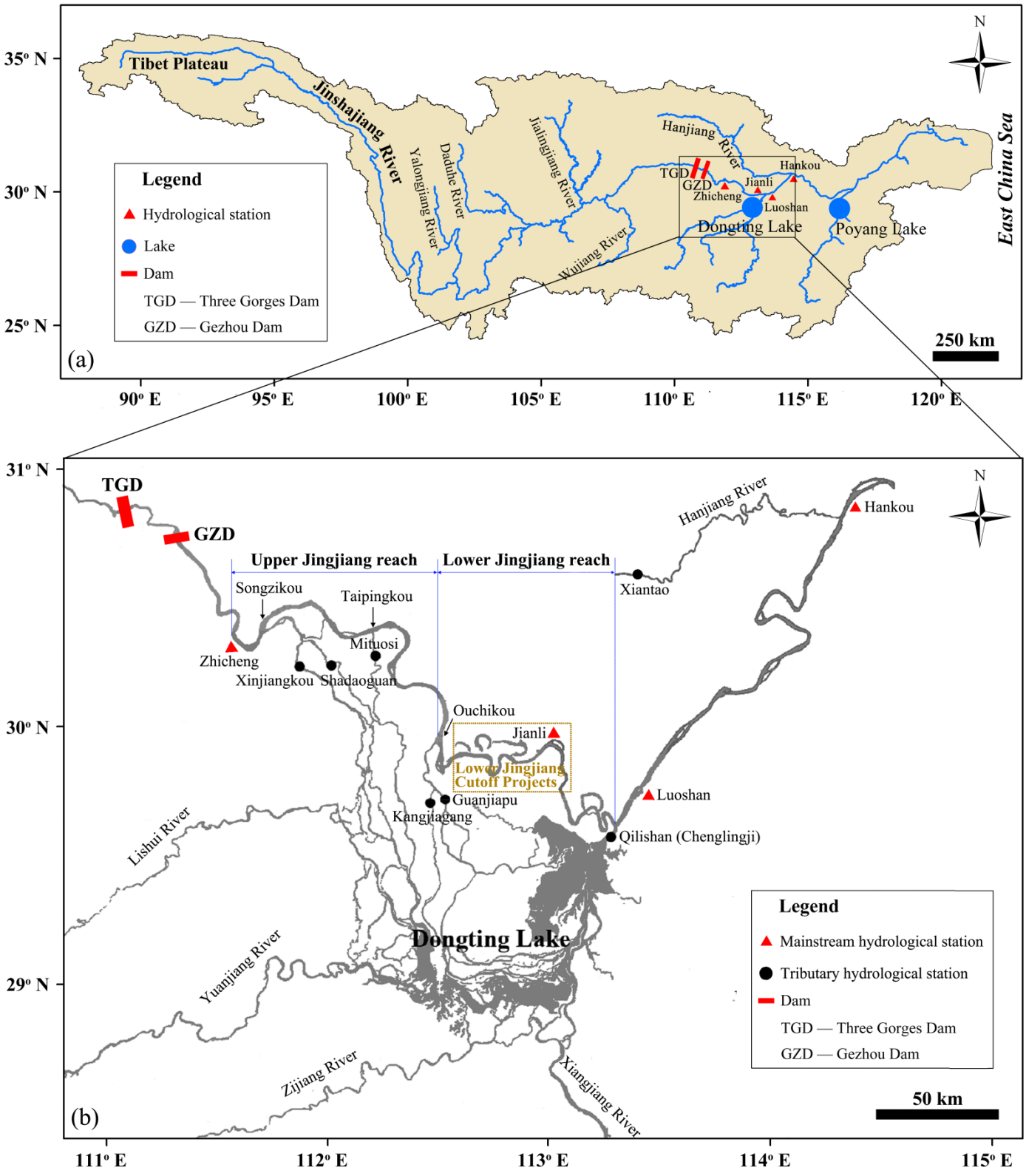


650
651

652 **Fig. 2**

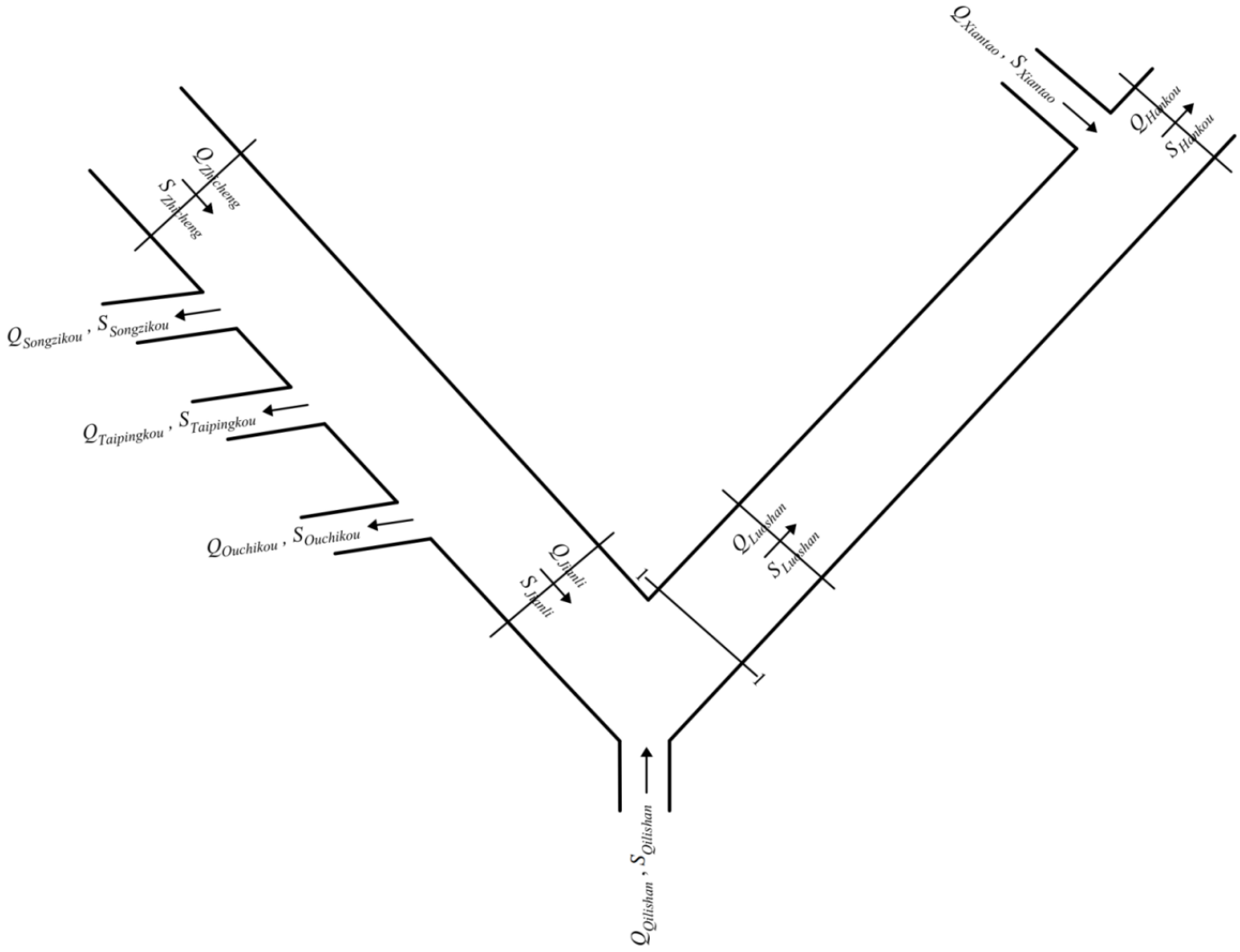


653

654

**Fig. 3**

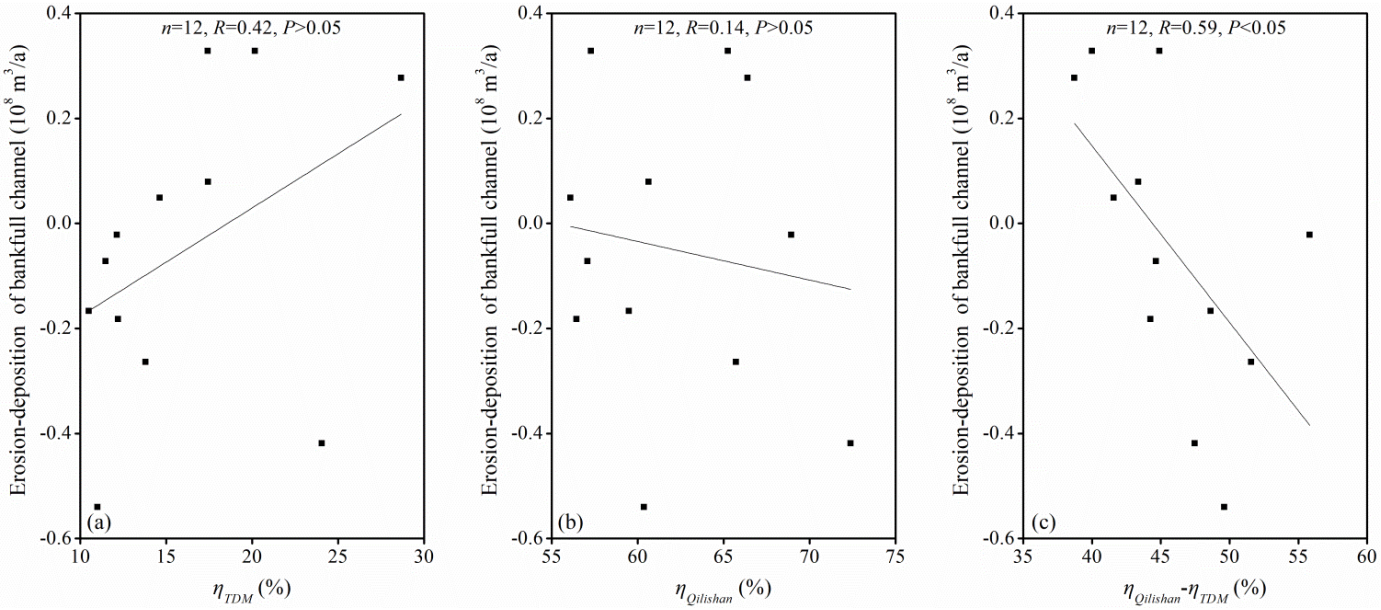
n=12, R=0.42, P>0.05
Erosion-deposition of bankfull channel ($10^8$ $m^3$/a)
(a)
$\eta_{TDM}$ (%)
n=12, R=0.14, P>0.05
(b)
$\eta_{Qilishan}$ (%)
n=12, R=0.59, P<0.05
(c)
$\eta_{Qilishan}$-$\eta_{TDM}$ (%)

**Fig. 4**

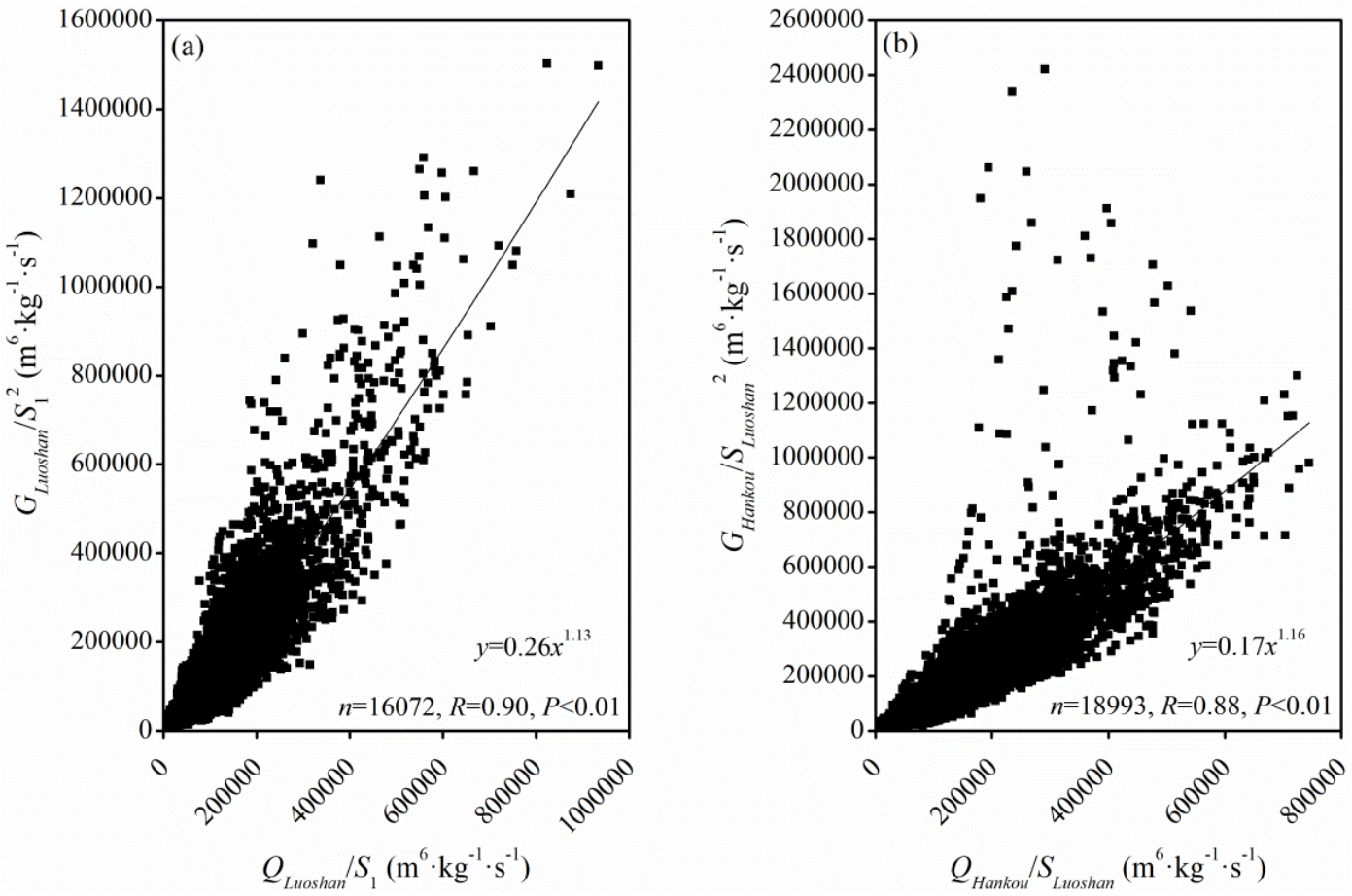
(a)
$G_{Luoshan}/S_1^2$ (m$^6$·kg$^{-1}$·s$^{-1}$)
$Q_{Luoshan}/S_1$ (m$^6$·kg$^{-1}$·s$^{-1}$)
$y$=0.26$x^{1.13}$
$n$=16072, $R$=0.90, $P$<0.01
(b)
$G_{Hankou}/S_{Luoshan}^2$ (m$^6$·kg$^{-1}$·s$^{-1}$)
$Q_{Hankou}/S_{Luoshan}$ (m$^6$·kg$^{-1}$·s$^{-1}$)
$y$=0.17$x^{1.16}$
$n$=18993, $R$=0.88, $P$<0.01

**Fig. 5**

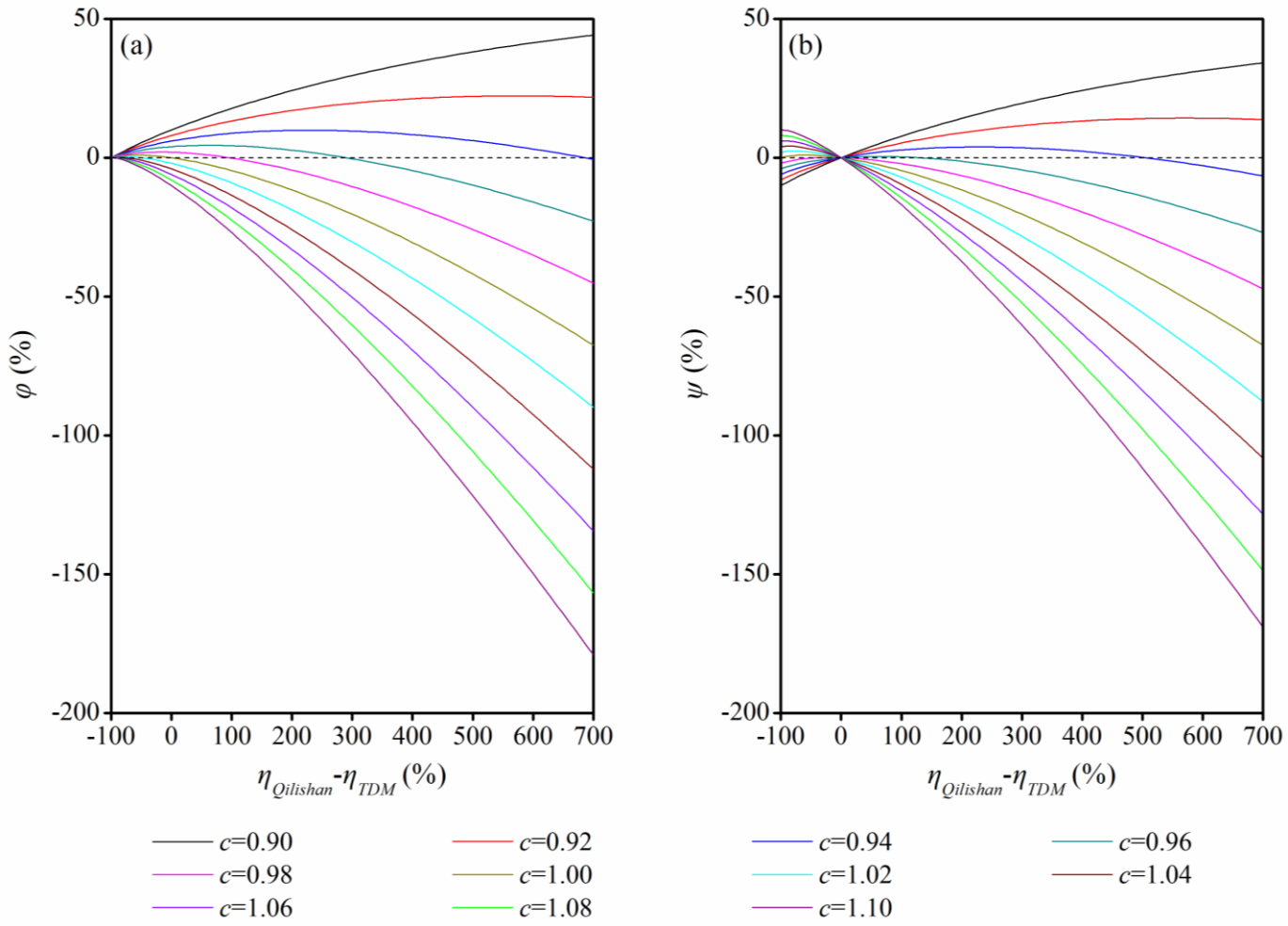
(a)
(b)
φ (%)
ψ (%)
$\eta_{Qilishan}$-$\eta_{TDM}$ (%)
50
0
-50
-100
-150
-200
-100
0
100
200
300
400
500
600
700
c=0.90
c=0.92
c=0.94
c=0.96
c=0.98
c=1.00
c=1.02
c=1.04
c=1.06
c=1.08
c=1.10

664 **Fig. 6**

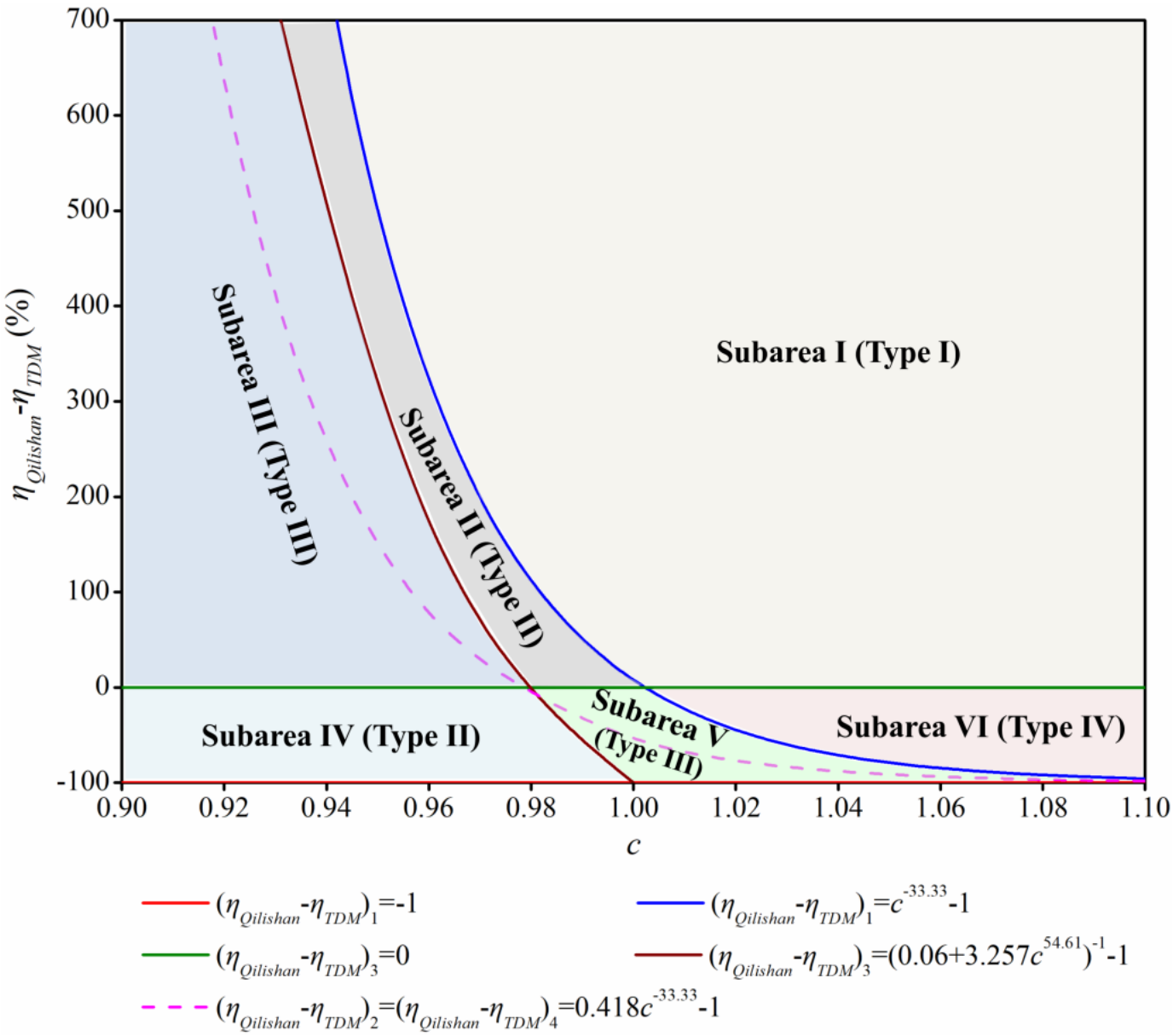


665

666

**Fig. 7**

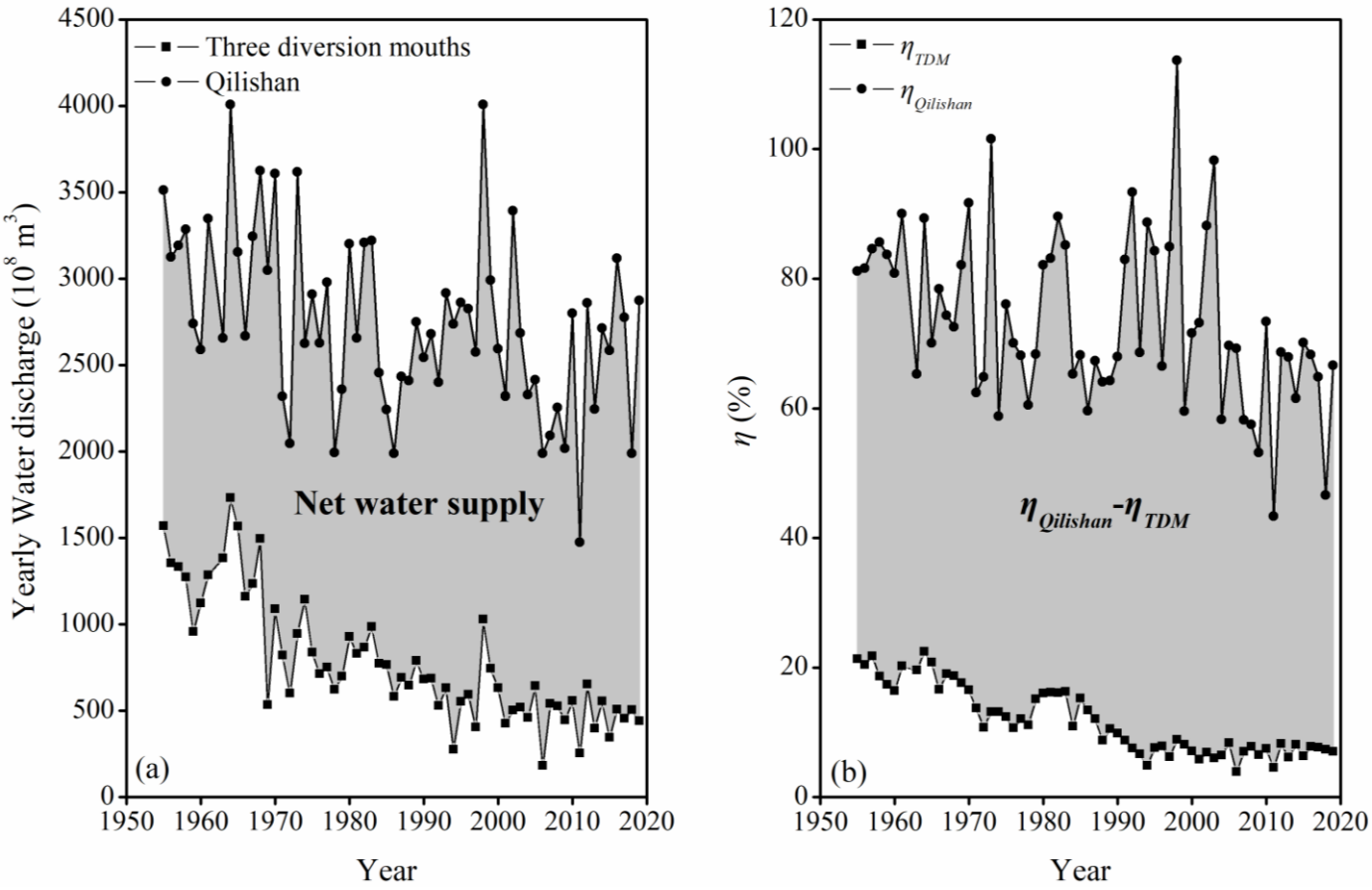
Three diversion mouths
Qilishan
Net water supply
Yearly Water discharge ($10^8$ $m^3$)
Year
(a)
$\eta_{TDM}$
$\eta_{Qilishan}$
$\eta_{Qilishan}$-$\eta_{TDM}$
$\eta$ (%)
Year
(b)

**Table 1**

Empirical formulae for $\varphi$, $\psi$, $\varphi_m$, $\psi_m$, and critical values of $\eta_{Qilishan}$-$\eta_{TDM}$ in terms of $c$ and $\eta_{Qilishan}$-$\eta_{TDM}$.

| Subject | | Formula/Value |
|---|---|---|
| Erosion-deposition | $\varphi$ | $\left[1+\left(\eta_{Qlishan}-\eta_{TDO}\right)\right]^{1.13}-c\left[1+\left(\eta_{Qilishan}-\eta_{TDO}\right)\right]^{1.16}$ |
| | $\varphi_m$ | $0.010c^{-37.67}$ |
| | $(\eta_{Qilishan}$-$\eta_{TDM})_1$ | -1 or $(c^{-33.33}-1)$ |
| | $(\eta_{Qilishan}$-$\eta_{TDM})_2$ | $0.418c^{-33.33}-1$ |
| Erosion-deposition promotion | $\psi$ | $\left\{\left[1+\left(\eta_{Qilishan}-\eta_{TDO}\right)\right]^{1.13}-1\right\}+c\left\{1-\left[1+\left(\eta_{Qilishan}-\eta_{TDO}\right)\right]^{1.16}\right\}$ |
| | $\psi_m$ | $0.010c^{-37.67}+c-1$ |
| | $(\eta_{Qilishan}$-$\eta_{TDM})_3$ | 0 or $\left[\left(0.06+3.257c^{54.61}\right)^{-1}-1\right]$ |
| | $(\eta_{Qilishan}$-$\eta_{TDM})_4$ | $0.418c^{-33.33}-1$ |

**Table 2**

Multi-year average variables related to river-lake water exchange and erosion-deposition (and its promotion) in the Luoshan-Hankou reach.

| Period | $\eta_{Qilishan}$-$\eta_{TDM}$ (%) | $c$ | $T$[a] ($10^8$ t/a) | $\Delta G_{Luoshan\text{-}Hankou}$ ($10^8$ t/a) | $\varphi$ (%) | $\delta$ ($10^8$ t/a) | $\psi$ (%) |
|---|---|---|---|---|---|---|---|
| 1959-1966 | 60.00 | 0.98 | 0.37 | 0.43 | 14.73 | -0.18 | -6.00 |
| 1966-1981 | 58.59 | 1.02 | 0.06 | -0.01 | -0.28 | -0.35 | -9.68 |
| 1981-1986 | 60.48 | 0.98 | 0.44 | 0.47 | 11.69 | -0.39 | -9.72 |
| 1986-2003 | 69.45 | 1.00 | -0.18 | -0.26 | -9.89 | -0.34 | -12.77 |
| 2003-2008 | 61.92 | 1.01 | -0.10 | -0.07 | -6.93 | -0.11 | -11.09 |
| 2008-2019 | 56.15 | 1.02 | -0.11 | -0.13 | -20.31 | -0.05 | -7.28 |
| 1959-2019 | 61.20 | 1.00 | 0.02 | -0.02 | -1.83 | -0.23 | -9.42 |
| Linear regression equation: $\varphi$=-0.10($\eta_{Qilishan}$-$\eta_{TDM}$)+0.04; $n$=7, $R$=0.03, $P$>0.05 | | | | | $\varphi$=-5.88$c$+5.87; $n$=7, $R$=0.81, $P$<0.05 | | |
| $\psi$=-0.42($\eta_{Qilishan}$-$\eta_{TDM}$)+0.16; $n$=7, $R$=0.77, $P$<0.05 | | | | | $\psi$=-0.25$c$+0.15; $n$=7, $R$=0.18, $P$>0.05 | | |

[a] $T$ represents net erosion-deposition rate of bankfull channel of the actual Luoshan-Hankou reach provided by the Changjiang Water Resources Commission.